Reprint

Aug 1986

NO.46

CI/SfB (M5)

UDC 53.087:536.2

# ENGINEERING APPLICATION OF HEAT FLUX SENSORS IN BUILDINGS -THE SENSOR AND ITS BEHAVIOR

H.A. Trethowen

Reprinted from *ASTM Special Technical Testing Publication 885* (1986)



BUILDING RESEARCH ASSOCIATION OF NEW ZEALAND

*Harold A. Trethowen*[1]

Authorized Reprint from
Special Technical Testing Publication 885
Copyright
American Society for Testing and Materials
1916 Race Street. Philadelphia, PA 19103
1986

# Engineering Application of Heat Flux Sensors in Buildings—The Sensor and Its Behavior

**REFERENCE:** Trethowen, H. A., "**Engineering Application of Heat Flux Sensors in Buildings—The Sensor and Its Behavior,**" *Building Applications of Heat Flux Transducers, ASTM STP 885*, E. Bales, M. Bomberg, and G. E. Courville, Eds., American Society for Testing and Materials, Philadelphia, 1985, pp. 9-24.

**ABSTRACT:** The factors affecting the measurement accuracy of (perfectly calibrated) heat flux sensors in buildings are discussed. A preliminary attempt is made to quantify this measurement error using dimensionless parameters. This attempt indicates that the method offers some promise and that some previously little-discussed items, such as the absolute size of the sensor, may have a great effect on the accuracy. An additional heat flux sensor is described, and a simple calibration method using a heater foil is outlined.

**KEY WORDS:** surface heat transmission, heat flux metering, buildings, sensor accuracy, sensor calibration, heat flux transducers

This paper describes the sensor used in the survey discussed in another paper in this publication [*1*] and investigates its application.

Since heat flux sensors (HFSs) were described in 1924 by Nicholls [*2*], a huge variety of HFS devices have been used. The two basic reasons seem to be that (*a*) the HFS properties required for different purposes vary widely, and (*b*) the designers of HFS devices have lacked adequate reference material on the real minimum properties needed. Both reasons have clearly influenced many HFS designs.

HFS devices for building heat flux are perceived essentially as devices to represent one-dimensional heat flux by reporting the temperature difference between two surfaces separated by a known and substantially constant thermal resistance. It is the duty of the user to ensure that the heat flux so reported will approximate that desired.

[1] Head, Components Division, Building Research Association of New Zealand, Porirua, New Zealand.

HFS devices can be mounted in three basic ways:

1. Embedded—The HFS is embedded within a slab of (unrelated) material in which the heat flux is to be determined.
2. Sandwiched—The HFS is built into a portion of a large, thin layer having the same thermal properties as the sensor and is then sandwiched between other layers.
3. Surface mounted—The HFS is mounted on an available surface, with or without edge guards. The surface may be a visible surface of the test piece or an internal surface exposed to an internal cavity.

All three ways can be used either for the application or for the calibration of the devices. For a mature technology, the application procedure would be independent of the calibration technique. Thus, it is necessary to be able to separate the intrinsic from the extrinsic (application-dependent) properties of HFS devices. Calibration procedures need to establish the intrinsic properties. An application technology needs to show how to use the devices and interpret their readings.

The "embedded" method has been comprehensively examined by Schwerdtfeger [*3*], who showed that the main factors affecting reliable performance are the relative conductivities of the sensor and parent materials and the sensor dimensions. It would not be difficult to implement a three-dimensional sensor in this situation by detecting three temperature differences across a cuboid sensor. The "sandwiched" method is usually encountered in laboratory thermal conductance measurements. The principal goal in this case is near-homogeneity of thermal properties between the sensor and its surroundings, to preserve the one-dimensional nature of the heat flows. It is not important whether both sensor and surroundings have high or low resistance. Detailed requirements have been presented in documents such as the ASTM Test for Steady-State Thermal Transmission Properties by Means of the Heat Flow Meter (C 518-76).

The "surface-mounted" method is the most complex, mainly because it is the least ideal in that it does not give full control of the measurement process. However, it is the most important method from an engineering viewpoint, as it is often the only available method of measuring heat flows in real buildings. The complexity arises precisely because the disturbing factors cannot be designed out but, instead, have to be assessed and controlled.

This paper is concerned solely with the "surface-mounted" method.

## Properties of Surface-Mounted HFSs

The objective is to ensure that the heat fluxes indicated by an HFS device can be reliably translated to the heat fluxes that would have occurred in the absence of the sensor. The first step is to clarify which properties are intrinsic to the sensor and which are a function of the application. The second step is to establish the behavior of the sensor in its expected application. This has been done here principally through finite difference modeling, and the modeling results are then compared with laboratory experiences.

The total heat flux in the region of the sensor is reduced because of the additional local thermal resistance. Some of this reduced heat flux spills around the edges of the sensor. The sizes of these two influences are a complex function of the items in Table 1.

Consider two examples from the sensor described in Fig. 1, intended for application in a large survey of *in situ* $R$-values in occupied houses. Figure 2 illustrates the simulated heat flow patterns in a typical application. For the case illustrated, the calculated difference between the indicated heat flux, $Q_i$, and the undisturbed heat flux, $Q_0$, was about 6% as a result of increased local thermal resistance, and a further 7% from edge spill. About two thirds of the edge spill took place in the 10-mm gypsum, and two thirds of the rest occurred in the top one third of the insulation. For an uninsulated wall, the difference between $Q_i$ and $Q_0$ was 25% from increased local resistance and only 5% from edge spill. This illustrates that edge spill can be a less significant contributor.

## The Performance of Surface Heat Flux Sensors

There are at least eight independent variables that affect the measurement error of a surface-mounted HFS, even for indoor use. This is too many to handle, and some way of compressing the problem must be found. The surface HFS problem is a specific case of a wider heat transfer problem, sometimes called the "insulating rug" problem because of the situation of a rug or furniture item on a heated floor, and is encountered in a variety of situations in buildings. It has some peculiar properties, one being that for a number

TABLE 1—*Schedule of intrinsic and extrinsic properties of surface heat flux sensors.*

| Intrinsic Properties | Extrinsic Properties |
|---|---|
| Sensitivity | surface resistance |
| Series thermal resistance | contact resistance |
| Size and thickness | thermal conductance of substrate |
| Lateral conductance | inhomogeneity in element measured, for example, thermal bridging |
| Radiation color | |
| Mechanical properties, for example, flatness, robustness | |
| Stability, for example, aging | |
| Purity, that is, response to factors other than heat flux, such as absolute temperature, clamping pressure, electrical/magnetic noise | |
| Edge guarding (in-built) | edge guarding (add-on) |
| Response time in standard conditions | response time *in situ* |

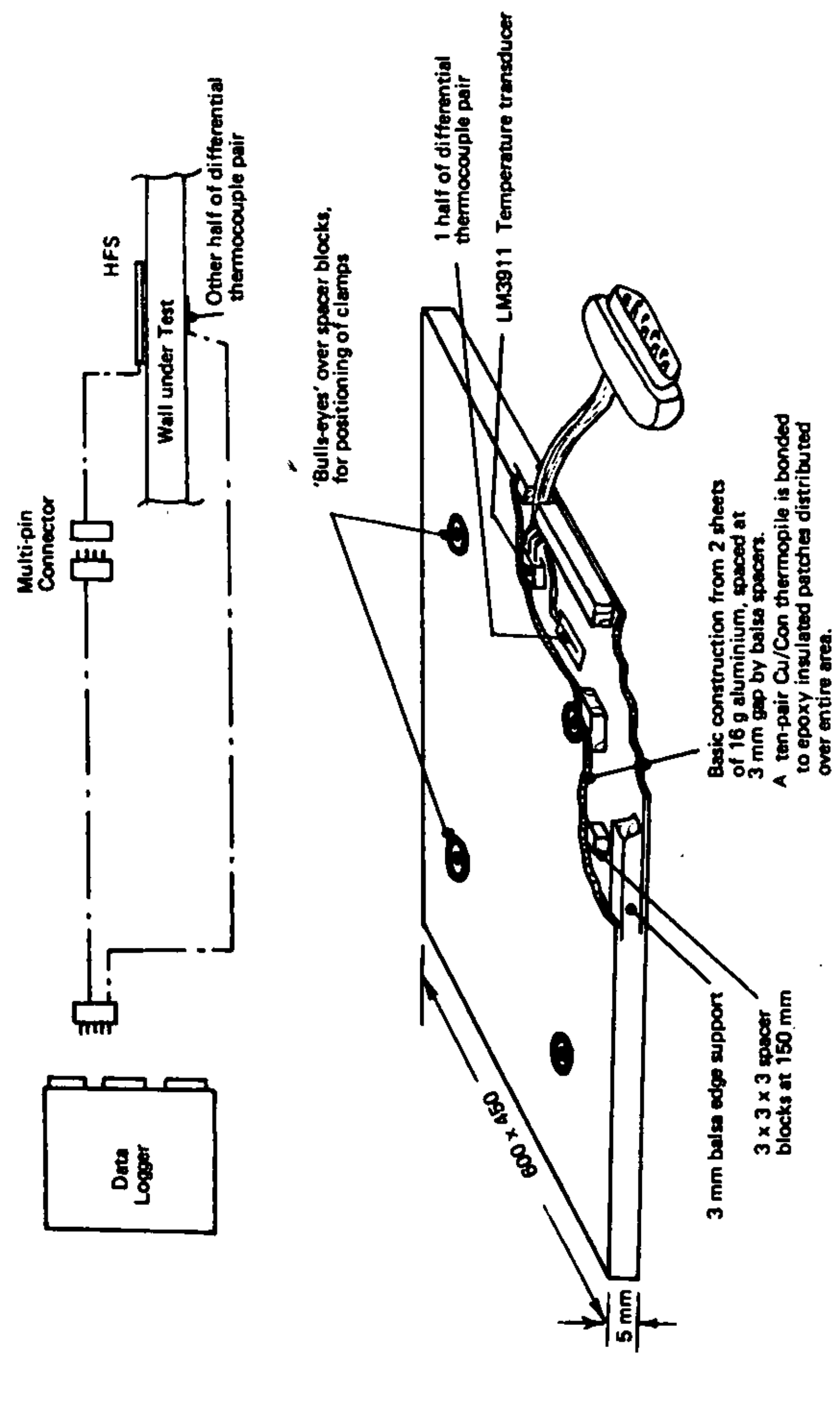


FIG. 1—*Construction details of a robust heat flux sensor for an* R-*value survey. (Note: This sensor is painted on both exterior surfaces and has unpainted internal surfaces.)*

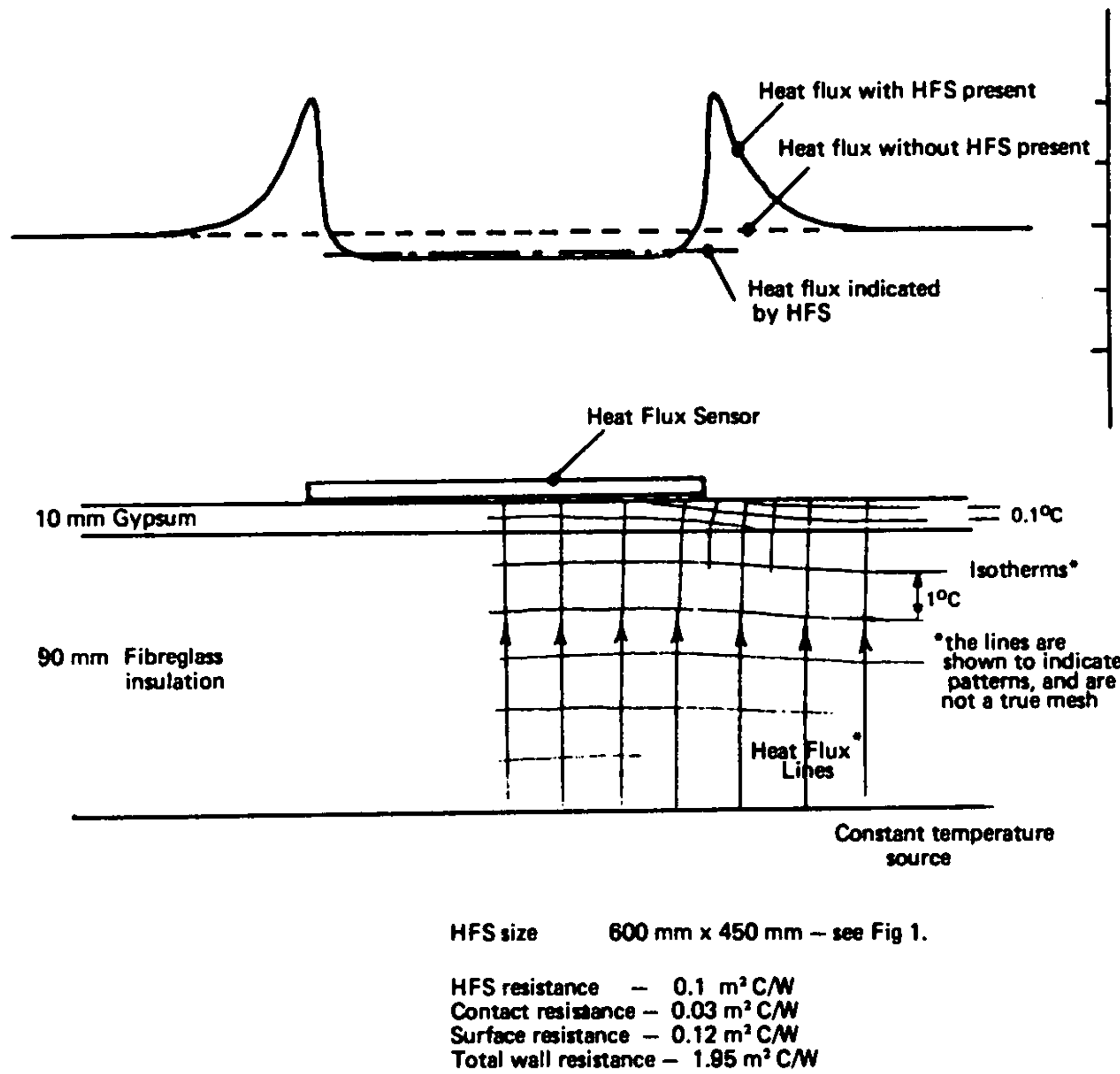


FIG. 2—*Heat flow around a heat flux sensor (see Fig. 1) from a finite difference model.*

of practical cases, the thermal disturbance created by the "insulating rug" can be as much a function of its size as of its insulation value. It is also mathematically intractable [*4*], and little aid is to be expected from analytical examination.

The usual resource in such intractable cases is to "normalize" the problem by identifying key dimensionless parameters. This appears to hold some promise for the surface HFS problem and has been partly developed in the following paragraphs for the HFS of Fig. 1. The principal tool has been finite-difference modeling. Some indicative laboratory tests were carried out under not particularly tightly controlled conditions, which produced results generally consistent with the model (see Fig. 3).

The finite-difference model was an explicit, time-dependent one, which was run to equilibrium to give steady-state heat flows. It was written to deal specifically with the physical form in Fig. 2, in three dimensions. The algorithms were based on Ref 5, with nodes at the element centroids. The Biot-number method was used to deal with boundaries.

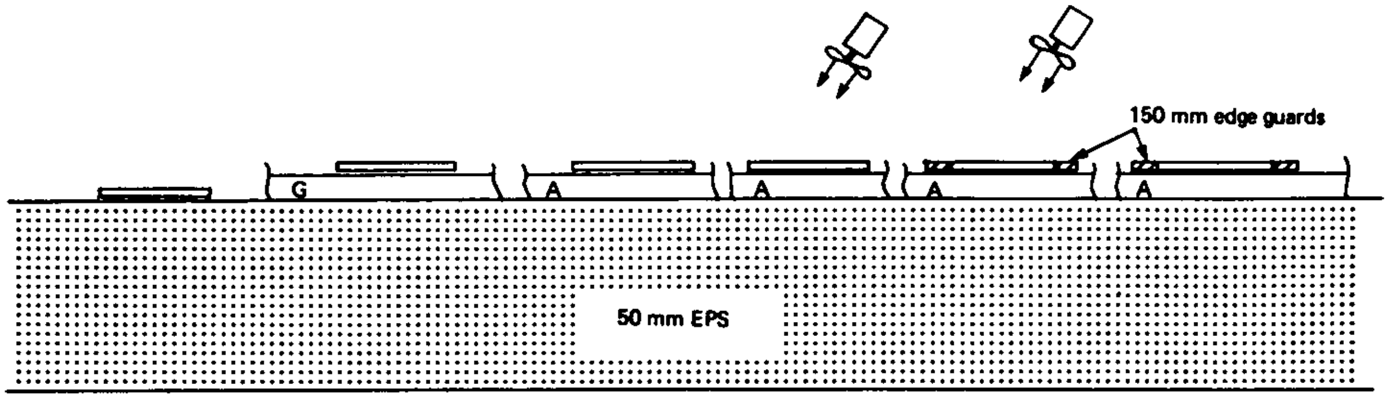


| Case | 1 | 2 | 3 | 4 | 5 | 6 | Assumed Confidence Interval |
|---|---|---|---|---|---|---|---|
| Airspeed at HFS | "Still" | "Still" | "Still" | 2 m/s | 2m/s | "Still" | |
| Observed error | 0 | 6% | 10% | 14% | 2% | 3% | ± 2 |
| Predicted error | 0 | 7% | 8% | 11% | 1% | 3% | |

a comparison of observed and predicted error in HFS-indicated heat flux, relative to case 1, for HFS of Fig. 1, fully taped all edges.

G = 10 mm Gypsum plasterboard
A = 6 mm Asbestos-cement board
EPS = 50 mm expanded polystyrene

Panel size 1.6 m x 1.2 m.

FIG. 3—*Laboratory-measured heat flux sensor error for several conditions, compared with finite-difference predictions.*

Typical nodal equations are given in Eq 1*a* and 1*b*. The limitations of the explicit method were handled by using small time steps (typically 1 min) based on stability conditions, which were tested for each boundary before simulation began. The space mesh was fixed at 10-mm cubes for the surface layer and 30-mm cubes for the insulation. The heat flux meter of Fig. 1 was modeled as two isothermal elements. The physical model was a one-quarter segment of a 1 by 1-m wall, and the heat flux sensor dimensions were kept to half of this or less, that is, to a maximum of 500-mm square. The heat flow was forced to be zero over all the edges of the model, and the surface heat flows were treated as simple heat flow resistance paths, taking air and radiant environment temperatures to be equal.

Within a material

$$\Delta T_p = F_0(T_n + T_s + T_e + T_w + T_u + T_d - 6T_p) \qquad (1a)$$

At an interface or surface

$$\Delta T_p = F_0[T_n + T_s + T_e + T_w + T_u + 2B_iT_d - (5 + 2B_i)T_p] \qquad (1b)$$

where

$T_p$ = temperature at point $p$,
$\Delta T_p$ = change in $T_p$ over one time step,
$F_0$ = Fourier number, and
$B_i$ = Biot number.

$T_n$, $T_s$, $T_e$, $T_w$, $T_u$, and $T_d$ are current temperatures in axially adjacent elements.

This modeling showed several clear conclusions, some apparently differing from those of previous authors such as Johannesson [6]. The dimensionless parameters that empirically were found to best fit the data were the two ratios $(R_m + R_c)/R_T$ and $k(R_m + R_c)/L$. For the conditions examined, the surface resistance and the conductivity of the surface layer of the wall were not strong factors.

The results of 50 or so modeling runs for the sensor of Fig. 1 are presented in Fig. 4, and these conform quite well to the formulas in Eqs 2*a* and 2*b*, with Eq 2*b* being the obvious relation in which large enough edge guards are present.

Unguarded
$$\frac{Q_0 - Q_i}{Q_0} = 0.75\left[\frac{k(R_m + R_c)(R_m + R_c)}{L \cdot R_T}\right]^{0.43} \qquad (2a)$$

Edge guarded
$$\frac{Q_0 - Q_i}{Q_0} = \frac{(R_m + R_c)}{(R_m + R_c) + R_T} \qquad (2b)$$

| Item | Code | Symbol | Explored Range | 'Home' Value |
|---|---|---|---|---|
| 'Home Case' | - | ● | - | - |
| Total Wall Resistance varied | $R_T$ | ○ | 0.3-3.4 m²C/W | 2.0 m²C/W |
| Surface layer conductivity varied | $k_s$ | □ | 0.05-1.3 W/mC | 0.16 W/mC |
| HFS + Contact resistance varied | $R_m + R_c$ | △ | 0.03-0.13 m²C/W | 0.13 m²C/W |
| Surface Resistance varied | $R_s$ | ▽ | 0.03-0.17 m²C/W | 0.12 m²C/W |
| HFS edge length (square) varied | L | ◇ | 100-500 mm | 500 mm |
| Edge guard present | E | ε | 0-300 mm | 0 mm |

a dot within a symbol indicates that one or more other variables also changed

$Q_o$ = undisturbed heat flow
$Q_i$ = indicated heat flow
k = 1.0

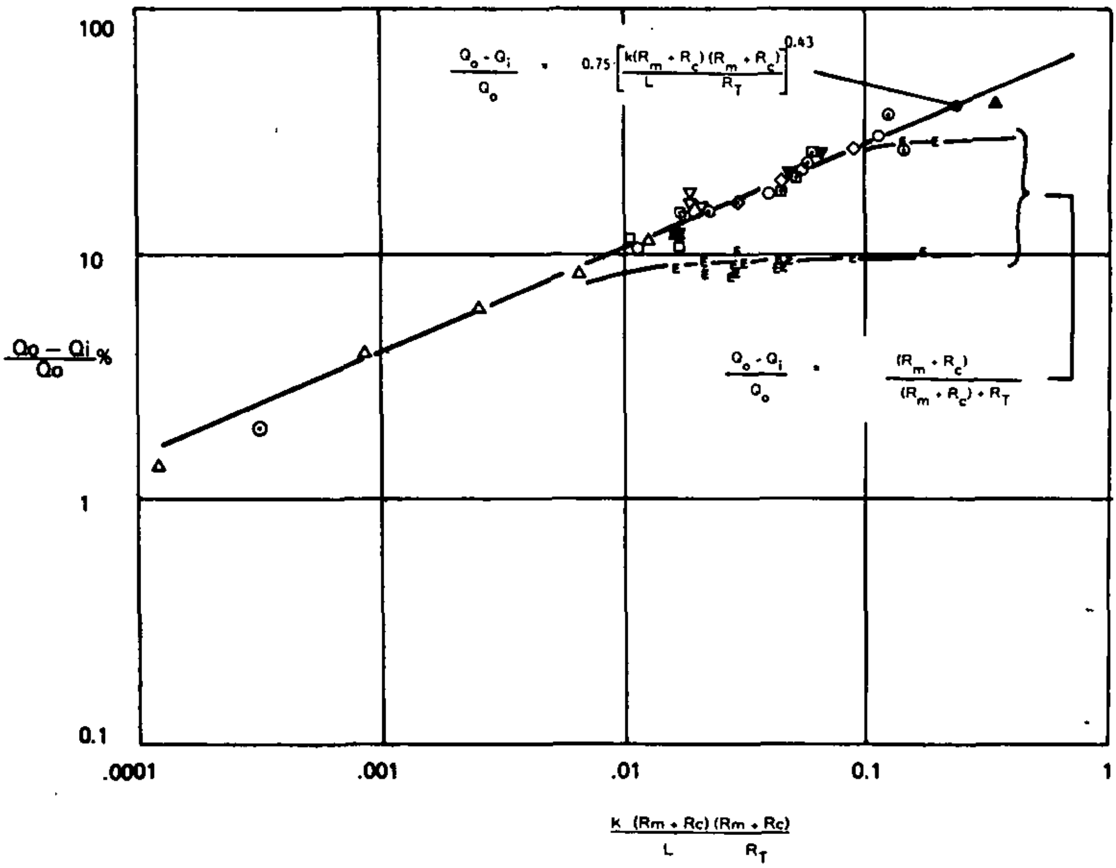


Note: All data from 3-dimensional finite difference model

FIG. 4—*A paramaterization of heat flux sensor output error.*

where

$R_T$ = thermal resistance of the test wall,
$R_m$ = thermal resistance of the HFS,
$R_c$ = contact resistance,
$L$ = edge length of the HFS (assumed square),
($k$ = thermal conductivity = 1.0),
$Q_i$ = heat flux indicated by a perfectly calibrated HFS, and
$Q_0$ = undisturbed heat flux.

This work is still unfinished, mainly with respect to the conductivity, $k$, which is present here as a dummy to make the dimensions compatible. No real conductivity term in the model has the correct influence. One might expect the conductivity, $k_s$, of the surface layer of the wall to fit. The ratio, $k_s/L$, would then express the lateral resistance for heat to bypass a barrier of ($R_m$ + $R_c$). However, $k_s$ had far too small an effect, with both $k_s$ and the surface resistance, $R_s$, having approximately cube root influence compared with that of $L$ and $R_T$.

The implications for the design of HFS applications are made very obvious by formulas such as Eq 2. It should be noted that contact resistance, $R_c$, is typically 0.01 to 0.03 (corresponding to a mean contact gap of 0.1 to 0.3 mm) in buildng applications. Sensor resistance less than, perhaps, 0.03 therefore may be of little advantage unless special contact measures are taken. Big sensors have a clear advantage, and errors are smaller with better insulated walls.

The effect of edge guards was relatively simple. Quite narrow guards ($<100$ mm) were sufficient to invoke the situation of Eq 2*b*, and narrower guards can be approximated in Eq 2*a* by putting $L$ equal to the total size ($L$ + $2E$) of the HFS plus guards. If the guard is imperfect (that is, has a different resistance from the HFS), then Eq 1*b* will also be imperfect. This may occur, for instance, if the edge guard has different contact resistance from the HFS. The simulations indicated that the edge guard resistance must match the HFS very closely if high accuracy is sought.

The notable conclusion for the range of data examined here was the relative insensitivity of measurement error to conductivity, $k_s$, of the surface layer, and to surface resistance, $R_s$ A 2:1 increase in $k_s$ increased the error in a typical case from 12 to 14%, while a 2:1 increase in $R_s$ reduced the error from 12 to 10%. This insensitivity may be a feature of the choice of conditions examined here and may not be generally true.

There seems to be some hope that, with more investigation, relationships such as the formulas in Eqs 1*a* and 1*b* might be extended to cope with a wide variety of surface HFS applications (including, perhaps, other designs of HFS). Such relationships achieve two things: (*a*) they enable useful results to be obtained in the engineering world with imperfectly chosen equipment and (*b*) they aid the rational selection of the conditions required for a specific heat flux measurement task.

**Transients**

The response time constant of an HFS has both intrinsic and application-dependent parts. The first-order component of the time constant is the ratio of (mass × specific heat content)/(surface heat transfer coefficient). The former is an intrinsic sensor property; the latter is application dependent. The time constant will, therefore, be different for disturbances from each side of an HFS, and if exposed to changing wind, rain, or radiation conditions, the time constant will vary continuously with time. The concept of an intrinsic response time constant is, thus, not realistic (for example, in the way that there is an intrinsic sensitivity coefficient).

Nevertheless, for a restricted range of applications, an engineering approximation is possible. For instance, the service time constant of an HFS for internal use in sheltered conditions would be dominated by its internal properties and by the still-air heat transfer coefficient. A reasonable measure of the time constant could then be found by monitoring response unmounted to a step change of temperature under still-air conditions. The time constant, when mounted, will not be substantially shorter, since rapid changes will be initiated only on the exposed face.

The practical significance of the time constant is that transient changes shorter than this time will be heavily suppressed by the sensor. But slower changes will be responded to more or less totally. The sampling interval of HFS recording equipment should never be greater than the effective time constant, to avoid aliasing errors. Theoretical arguments indicate that an HFS device exposed to fluctuations faster than its response time will, nevertheless, respond accurately to the mean value heat flux underlying those fluctuations. We have verified this in stepwise computer simulation for the sensor depicted in Fig. 1.

The response time constants of HFS devices can range from less than 1 s to 10 min or more. Many commercial sensors seem to have fast response capability. This is not always an advantage, and users of HFS devices frequently report having to "damp" the sensors by placing metal shields over them to avoid rapid, apparently erratic, output variations.

When an HFS is initially placed on a test structure, its output may show large transients. After one or more times the HFS time constant, the HFS indication will rapidly approach the true local heat flux at the sensor. But this local heat flux may be grossly different from that in which there is no sensor. This difference will persist for a period greater than the dominant time constant of the wall (typically, 2 to 50 h) rather than that of the sensor (1 s to 10 min). The thermal resistance added by the sensor requires that the structure temperatures be redistributed, and this can occur only at the response rate of the structure. The properties of the HFS affect only the size of this redistribution and not its rate. The readings are not reliable until the redistribution is complete. An example is given in Fig. 5, which has a relatively slow HFS time constant of about 8 min and an unusually fast wall time constant of about 40 min. The HFS output rapidly begins to converge on the true heat flux after 10 to 20 min, but the readings nevertheless do not represent the undisturbed heat flow to a similar stage of reliability for 1½ h.

Once this initial stage is over, the response time of the measurement is dominated by the time constant of the HFS. The wall itself may show major storage processes, and these will be reliably reflected in the HFS output, provided they are significantly slower than the HFS time constant. Even if they are not, the HFS will reliably show the mean value of fast cycles. For example,

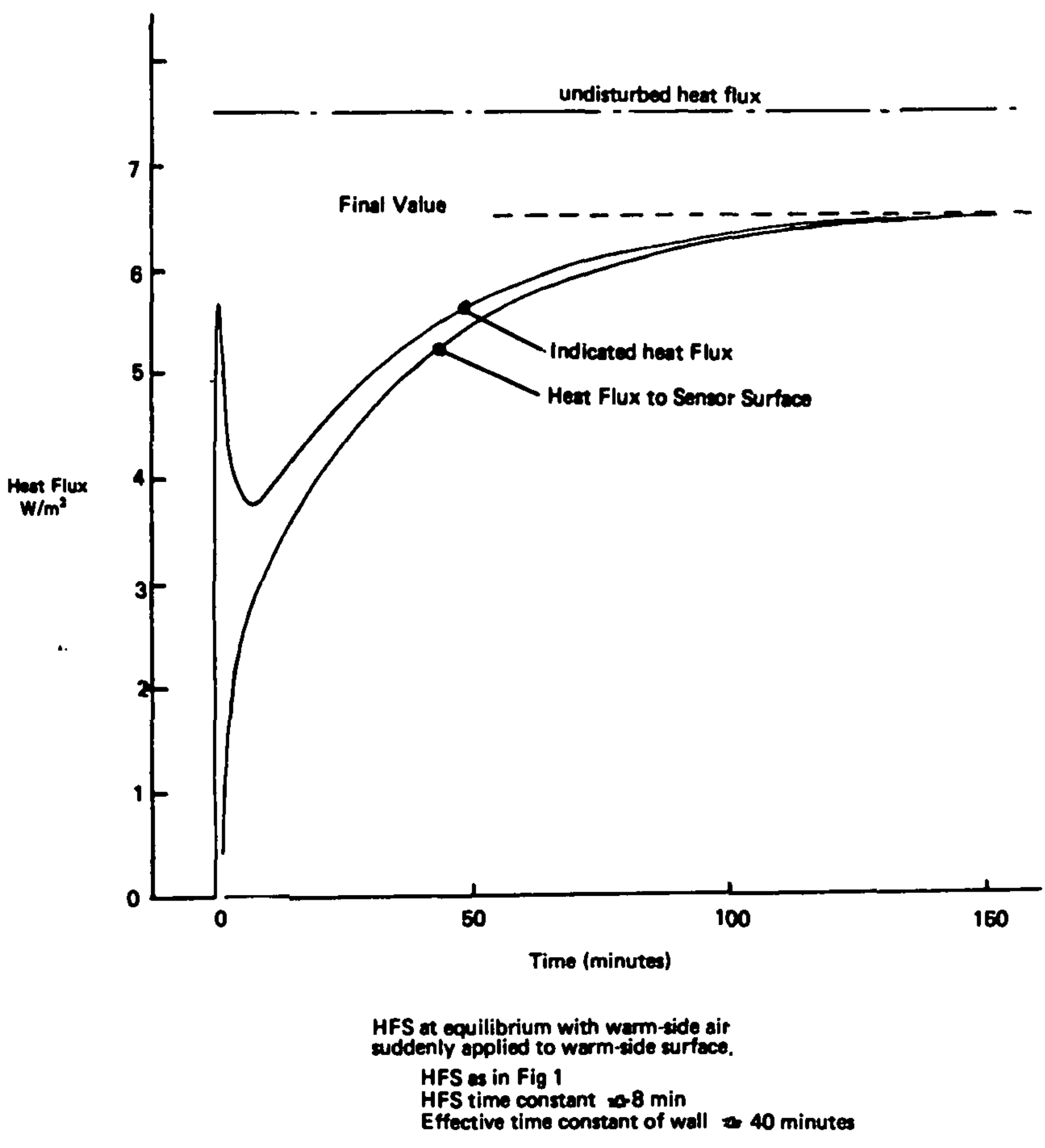


FIG. 5—*Predicted transient behavior on installation of a surface heat flux sensor.*

the response to a cyclic air temperature change of a 20-min period was simulated in the previous case. The indicated heat flux was 0.55 that of the undisturbed surface with a 36° phase lag, but the corresponding mean value over a cycle was within 0.2% of the correct value.

The heat flux indicated during slowly drifting temperature will usually be the true structure response, and not an artifact of the sensor. The heat flux may be far from the steady-state value.

### Calibration

One difficulty with surface HFS devices is the lack of any written guidance on their calibration and how this may differ from their apparent sensitivity in use. In this section, calibration is taken to mean a true or intrinsic "calibration," that is, the establishment of the function that relates output signal to heat flux through the sensor.

The guarded hot plate is a commonly used calibration apparatus. It is a well-established method which needs no further discussion here, except to point out one practical limitation. An accurate calibration requires either that the HFS have the same size as the hot plate or that its properties be known and matched with edge dummy fill. This may not always be feasible.

The initial calibration procedure used in this project was based on replicating the in-service conditions (see Fig. 6*a*). The view, then, was that not enough was known about the edge spill factors, and calibration for each substrate might be needed. The intrinsic sensitivity of the device would be given by calibration over an insulating substrate (such as expanded polystyrene).

This was later replaced by the "heating foil" calibration procedure illustrated in Fig. 6*b*. A pair of HFSs are clamped to the two sides of a heated foil. This method has several major advantages and should be considered as a candidate for a standard method for surface-mounted HFS devices, because of the following factors:

1. It gives both intrinsic sensitivity and response time constant.
2. It is relatively rapid.
3. It can readily be used, irrespective of the HFS size and internal properties.
4. It uses simple equipment and does not require special facilities (other than precision voltage measurement).
5. The requirements are readily definable and the results are consistent.

A disadvantage is that a single HFS cannot readily be calibrated by this method. A minimum of three sensors, nominally identical, are needed. Since each HFS may have slightly different heat flow resistance, the heat emitted by the heating foil does not necessarily divide equally through the two sensors. This problem can be easily overcome by measuring the sensors in each possible pairing of sets of three. The individual calibration constants can then be

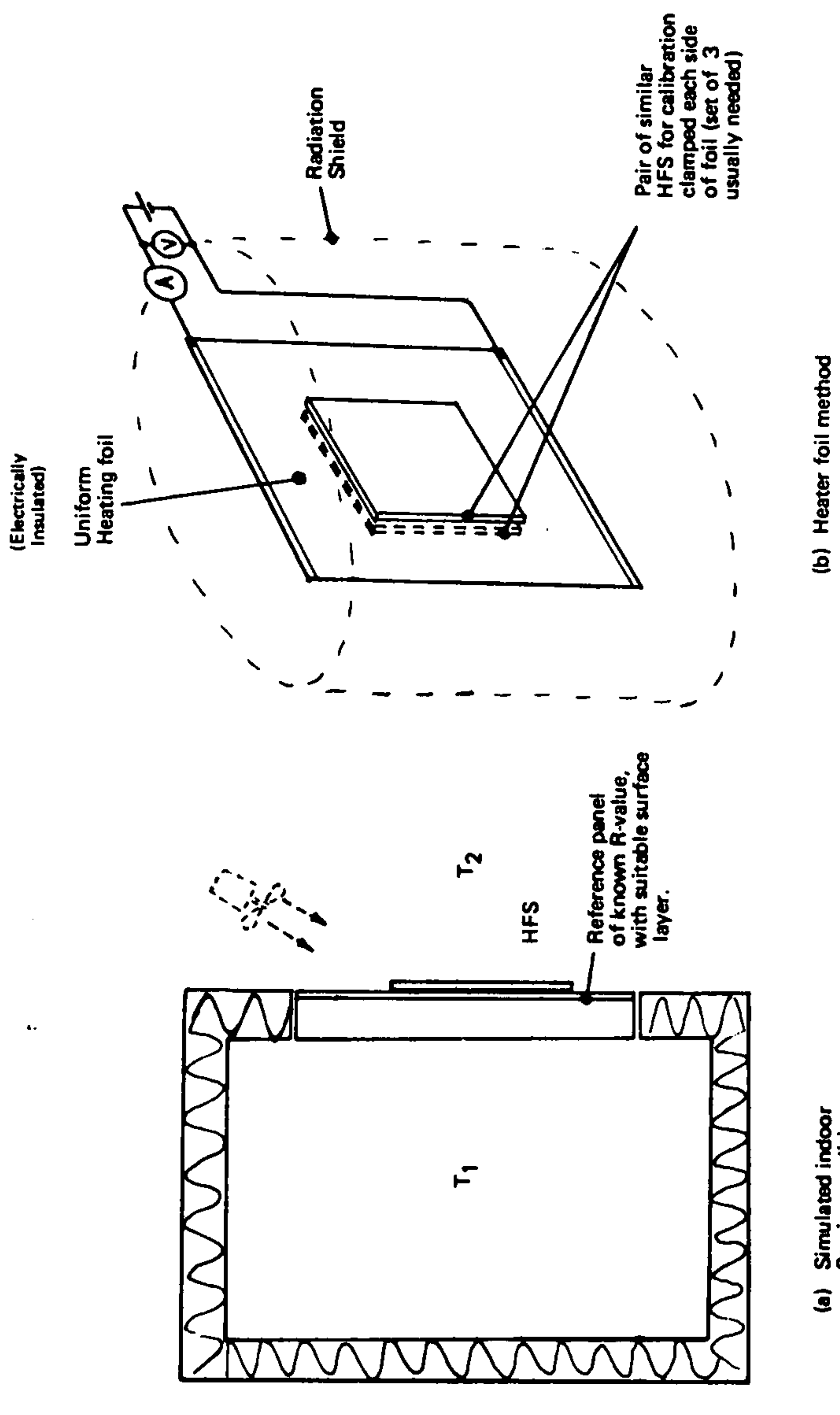


FIG. 6—*Two methods of investigating the calibration of surface heat flux sensors.*

found, making use of the uniformity of heat generation in the foil. The heat flux generation in the foil must be equal to the sum of losses for each side

$$
\begin{aligned}
\frac{Q_1}{A} &= K_a V_{a1} + K_b V_{b1} \\
\frac{Q_2}{A} &= \qquad\qquad K_b V_{b2} + K_c V_{c2} \\
\frac{Q_3}{A} &= K_a V_{a3} \qquad\qquad + K_c V_{c3}
\end{aligned}
\tag{3}
$$

where

$Q_1, Q_2, Q_3$ = total foil emission in Runs 1, 2, and 3, W,
$A$ = projected area of foil, $m^2$,
$V$ = output for subscript sensor, run, mV, and
$K_a, K_b, K_c$ = calibration constants for HFSs $a$, $b$, and $c$, $W/m^2 \cdot mV$.

From this set of equations, $K_a$, $K_b$, and $K_c$ can be readily found. If one or more temperature differences are measured, the individual thermal resistances of the sensors can also be found.

It has been our practice to calibrate in groups of four or five, so that several different estimates of $K$ can be found for each sensor. This has led to standard deviations in the estimates for each sensor of about 1% of the calibration constant.

It is necessary to surround the test with a simple radiation shield. Thermal asymmetry of even a good laboratory space can otherwise easily increase the standard deviation of measurement up to 3 to 5%.

## Field Measurement of *R*-Values

It is suggested that (*a*) HFS devices should never be directly exposed to sunshine but should be concealed below a sample of the parent surface and that (*b*) flux measurements for *R*-value determination should be made on the inside wall surface *only*.

The restriction to internal measurements immediately removes almost all of the problems of radiation color matching. It also brings the HFS into a region relatively free from short-term transients, and it stabilizes the operating temperature of the HFS so that its sensitivity is more constant. It makes mounting much easier. If the structure cavity is ventilated, the indoor mounting position will more successfully measure all the heat leaving the occupied space.

The advantages of indoor HFS mounting are so great that the alternative should be considered only if, for some reason, inside mounting is impossible.

In attempting to apply the foregoing principles to an HFS for application in a large-scale (about 100 houses) survey of in-service *R*-values, several further factors arose. Clearly, physical robustness was needed. It was also necessary that no damage or marks be left on interior finishes (thus, adhesive tapes and filler pastes were ruled out). Installation procedures also had to be compatible with production-line philosophy.

The sensor design shown in Fig. 1 was developed to satisfy the following criteria:

(*a*) physical robustness (including electrical connections),

(*b*) ease in clamping in place by nonmarking methods,

(*c*) adequate size to match typical framing spacing for (almost universal) timber frame construction, and also compatibility with concrete masonry or other building types,

(*d*) high lateral conductance to aid averaging,

(*e*) not-too-short response time,

(*f*) adequate signal output (ten-pair thermopile) (approximately 25 $W/m^2 \cdot mV$),

(*g*) series resistance ($\leq 0.1$ $m^2C/W$), and

(*h*) simplicity of construction.

Built into each HFS was a National Semiconductor LM3911 temperature transducer and one half of an indoor-surface/outdoor-surface differential thermocouple, on the wall-side surface of the sensor. All the mounting and electrical connection problems of those items on site were thus eliminated.

It is interesting that even though these sensors were handmade, the calibration coefficients varied from one to another by less than 10%.

Data obtained from this equipment allowed ready computation of mean *in situ R*-values, surface-to-surface, using the cumulative method described by Flanders [*7*]. These results showed maximum errors within ±10%.

## Conclusions

This paper offers comment on the calibration of heat flux sensors for surface application and on the engineering application of these devices to real buildings in nonideal circumstances.

A preliminary attempt using dimensionless parameters to formulate a general expression describing the measurement accuracy of HFS devices is offered.

## References

[*1*] Isaacs, N., "Engineering Application of Heat Flux Sensors in Buildings—Technical Note," this publication, pp. 122–128.

[*2*] Nicholls, P., "Measuring Heat Transmission in Building Structures and a Heat Transmis-

sion Meter," *Transactions of the American Society of Heating and Ventilating Engineers*, Paper 685, 1924.

[3] Schwerdtfeger, P., "The Measurement of Heat Flow in the Ground and the Theory of Heat Flux Meters," Technical Report 232, U.S. Army Cold Regions Research and Engineering Laboratory, Hanover, NH, 1970.

[4] Weir, G., "Insulating Circular Rugs," *Journal of the Australian Mathematical Society, Series B*, Vol. 24, 1983, pp. 359–365.

[5] Croft, D. and Lilley, D., *Heat Transfer Calculations Using Finite Difference Equations*, Applied Science Publishers, London, 1977.

[6] Johannesson, G., "Preliminary Report on the Use of Heat Flow Meters in Building Construction," Workshop Meeting of the W40 Commission of the Conseil International du Batiment, Washington, May 1976.

[7] Flanders, S., "Toward *in Situ* Building *R*-Value Measurement," U.S. Army Cold Regions Research and Engineering Laboratory, Hanover, NH, 1982.

B12139
0018685
1986
Engineering application o
f heat flux sensors in bu

BUILDING RESEARCH ASSOCIATION OF NEW ZEALAND INC.
HEAD OFFICE AND LIBRARY, MOONSHINE ROAD, JUDGEFORD.

The Building Research Association of New Zealand is an industry-backed, independent research and testing organisation set up to acquire, apply and distribute knowledge about building which will benefit the industry and through it the community at large.

Postal Address BRANZ, Private Bag, Porirua

branz

ISSN 0111–7459